

The Post-Newtonian Approximation of the Rigidly Rotating Disc of Dust to Arbitrary Order

D. Petroff and R. Meinel
 Theoretisch-Physikalisches Institut
 University of Jena
 Max-Wien-Platz 1, 07743 Jena, Germany
 D.Petroff@tpi.uni-jena.de

October 31, 2018

Abstract

Using the analytic, global solution for the rigidly rotating disc of dust as a starting point, an iteration scheme is presented for the calculation of an arbitrary coefficient in the post-Newtonian (PN) approximation of this solution. The coefficients were explicitly calculated up to the 12th PN level and are listed in this paper up to the 4th PN level. The convergence of the series is discussed and the approximation is found to be reliable even in highly relativistic cases. Finally, the ergospheres are calculated at increasing orders of the approximation and for increasingly relativistic situations.

1 Introduction

The study of a three-dimensional, arbitrarily rotating fluid in general relativity cannot but rely on the use of numerical computation for its results. An important step along the way toward a proper application of numerical methods and toward an in-depth understanding of numerical results is the rigorous consideration of a simpler, but related, problem. Neugebauer and Meinel undertook this task in modelling a uniformly rotating disc of dust. The corresponding analytic, global solution to Einstein's field equations, which was worked out in the series of papers [1], [2] and [3] by utilizing the 'inverse scattering method' known from soliton theory, can be expressed using hyperelliptic integrals.

In this paper, the above mentioned global solution will be used as a starting point from which to derive an iteration scheme for the calculation of an arbitrary term in the post-Newtonian (PN) expansion of the solution. Such an expansion amounts to the analytic analogue of numerical work presented by Bardeen and Wagoner [4] in a paper that handles the rotating disc in great detail.

Given that the global solution for the uniformly rotating disc of dust is known, the question arises as to why one would consider the problem using the PN

approximation. The reasons are threefold. First, the complex nature of the solution leads to fairly long computing times, particularly if the relativistic parameter μ is to be varied. Using the PN approximation, one could speed up calculations dramatically. Secondly, one is presented the rare opportunity to check the accuracy of numerical work against its analytic analogue, thus allowing one better to determine the limitations of these numerical techniques. Lastly, since one can obtain an arbitrary term in the PN expansion, one can look at the convergence of the series for various applications and, moreover, see if the approximation can be used to study relativistic phenomena, where its validity is not *a priori* clear.

2 The Global Solution

The form of the metric to be used here is taken directly from [1] and reads

$$ds^2 = e^{-2U} [e^{2k} (d\rho^2 + d\zeta^2) + \rho^2 d\varphi^2] - e^{2U} (dt + a d\varphi)^2 \quad (1)$$

in Weyl-Lewis-Papapetrou coordinates.¹ The metric represents a stationary, axially symmetric spacetime and the three metric functions U, k and a depend only on ρ, ζ , the relativistic parameter

$$\mu = \frac{2\Omega^2 \rho_0^2 e^{-2V_0}}{c^2} \quad (2)$$

and the coordinate radius of the disc ρ_0 . The other quantities appearing in eq. (2) are the constant angular velocity Ω and the “surface potential” $V_0 \equiv U(\rho=0, \zeta=0)$, which is closely related to the redshift at infinity. The relativistic parameter μ runs from $\mu = 0$ in the Newtonian limit through to $\mu = \mu_0 = 4.62 \dots$ in the extreme Kerr limit. The four-velocity of a particle in the disc has only two non-zero components: $u^t = e^{-V_0}$ and $u^\varphi = \Omega e^{-V_0}$ (both components are independent of the radial coordinate ρ). As mentioned above, the metric depends on only two parameters, whence the profile for the surface mass density $\sigma(\rho)$ cannot be chosen freely, but is instead automatically determined by these parameters, i.e. a disc chosen to have the values $\mu = \tilde{\mu}$ and $\rho_0 = \tilde{\rho}_0$ can have but one angular momentum \tilde{J} and but one total gravitational mass \tilde{M} and the matter will need to be distributed according to $\sigma(\rho)$ as given by eq. (23) in [2].² A specific example of a mass density profile will be presented in section 4.2.

The vacuum field equations are equivalent to the complex Ernst equation (see [5])

$$\Re(f) \Delta f = (\nabla f)^2 \quad \text{with} \quad f = e^{2U} + ib \quad (3)$$

$$\text{and } b_{,\rho} = -\frac{e^{4U}}{\rho} a_{,\zeta}, \quad b_{,\zeta} = \frac{e^{4U}}{\rho} a_{,\rho}. \quad (4)$$

¹Units have been chosen in which G and c are equal to one, except in eq. (2), where the factor c^2 was included to show explicitly the relation $\mu \propto 1/c^2$ for reasons to be discussed in section 4.1.

²One could just as easily have chosen to consider a disc of mass M' and angular momentum J' and would then have been automatically led to the values for μ, ρ_0 and $\sigma(\rho)$ corresponding to this situation.

The operators Δ and ∇ in the above equation are three-dimensional. Taking into account boundary conditions on the disc, an asymptotically flat solution can be found for the Ernst potential f , which suffices to determine all three metric functions since a can be found using eq. (4) and k is related to the other two functions via a line integral as well. The potential f is given by the expression

$$\begin{aligned} \ln(f) &= \int_0^{m_a} \frac{(X(m) - X_1)(X(m) - X_2)}{2X(m)W_1(m)} dm \\ &\quad + \int_0^{n_b} \frac{(X(n) - X_1)(X(n) - X_2)}{2X(n)W_1(n)} dn \\ &\quad - \int_{-i}^i \frac{H(X - X_1)(X - X_2)}{W} dX \end{aligned} \quad (5)$$

$$\equiv I_1 + I_2 - I_3 \quad (6)$$

with

$$W = W_1 W_2, \quad W_1 = -\sqrt{(X - \zeta/\rho_0)^2 + (\rho/\rho_0)^2}, \quad (7)$$

$$W_2 = \sqrt{\mu^{-2} + (1 + X^2)^2}, \quad H = \frac{\operatorname{arcsinh}(\mu[1 + X^2])}{\pi i}, \quad (8)$$

$$X_1 = -\sqrt{\frac{i - \mu}{\mu}} \quad \text{and} \quad X_2 = \sqrt{-\frac{i + \mu}{\mu}}. \quad (9)$$

A negative sign appearing before the root of a complex quantity indicates that the real part is to be chosen to be negative. What is meant by $X(m)$, $X(n)$, $W_1(m)$ and $W_1(n)$ in eq. (5) is that the variable substitution

$$X = -\sqrt{\frac{i \cosh(m)}{\mu} - 1} \quad \text{or} \quad X = \sqrt{\frac{-i \cosh(n)}{\mu} - 1} \quad (10)$$

is to be carried out. The endpoints of integration m_a and n_b can be determined from the Jacobi inversion problem

$$\int_0^{m_a} \frac{dm}{2X(m)W_1(m)} + \int_0^{n_b} \frac{dn}{2X(n)W_1(n)} = u \quad (11)$$

and

$$\int_0^{m_a} \frac{dm}{2W_1(m)} + \int_0^{n_b} \frac{dn}{2W_1(n)} = v \quad (12)$$

with

$$u = \int_{-i}^i \frac{H dX}{W} \quad \text{and} \quad v = \int_{-i}^i \frac{HX dX}{W} \quad (13)$$

and where the path of integration in eq. (13), as with the integral I_3 in eq. (6), is along the imaginary axis. The above equations, which can be found in [3],

differ from the ones presented there in three ways: 1) The expression for $\ln(f)$ was manipulated algebraically, making use of eqs. (11), (12) and (13). 2) In each of the integrals I_1 and I_2 , the aforementioned variable substitution was carried through. 3) The definition for W_2 in this paper differs from that of [3] by a factor μ .

In discussing the Newtonian limit of the solution in [3], Neugebauer and Meinel make note of the fact that the solutions can be expanded in a power series

$$f = 1 + \sum_{n=1}^{\infty} f_n \mu^{(n+1)/2} \quad (14)$$

such that the coefficients are elementary functions. The following section presents a method for determining these coefficients.

3 The Iteration Scheme

A comparison of eqs. (10) and (9) shows that

$$X(m=0) = X_1 \quad \text{and} \quad X(n=0) = X_2 \quad (15)$$

hold. This suggests the rearrangement of eqs. (11) and (12) to form

$$\int_0^{m_a} \frac{X(m) - X_2}{2X(m)W_1(m)} dm + \int_0^{n_b} \frac{X(n) - X_2}{2X(n)W_1(n)} dn = v - X_2 u, \quad (16)$$

$$\int_0^{m_a} \frac{X(m) - X_1}{2X(m)W_1(m)} dm + \int_0^{n_b} \frac{X(n) - X_1}{2X(n)W_1(n)} dn = v - X_1 u, \quad (17)$$

which serves to “decouple” the original equations. What is meant here by decoupling, is that an iteration scheme for the determination of m_a (or equivalently n_b) as a power series in μ does not require the simultaneous consideration of two equations in its ultimate step. Eq. (16) yields up the ultimate term for m_a and eq. (17) for n_b .

Expanding the integrands in eqs. (16) and (17) about the points $m=0$ and $n=0$ respectively, one is left with trivial integrals

$$\sum_{i=0}^{\infty} a_i \int_0^{m_a} m^{2i} dm + \sum_{i=1}^{\infty} c_i \int_0^{n_b} n^{2i} dn = v - X_2 u \quad (18)$$

$$\sum_{i=1}^{\infty} d_i \int_0^{m_a} m^{2i} dm + \sum_{i=0}^{\infty} b_i \int_0^{n_b} n^{2i} dn = v - X_1 u. \quad (19)$$

Making use of the fact that m_a and n_b are both of the order $\mathcal{O}(\mu)$,³ one can derive the following iteration formulae:

$$m_{ak} = \frac{1}{a_0} \left[(v_1 \mu^2 + \dots + v_k \mu^{2k}) - X_2 (u_1 \mu^2 + \dots + u_k \mu^{2k}) \right]$$

³This follows from eqs. (18) and (19) along with the fact that the coefficients a_i, b_i, c_i and d_i are all of the order $\mathcal{O}(\sqrt{\mu})$, that u and v are of the order $\mathcal{O}(\mu^2)$ and that X_1 and X_2 are of the order $\mathcal{O}(1/\sqrt{\mu})$.

$$\begin{aligned}
& \left. \begin{aligned}
& -a_1 \frac{m_{a_{k-1}}^3}{3} - a_2 \frac{m_{a_{k-2}}^5}{5} - \dots - a_{k-1} \frac{m_{a_1}^{2k-1}}{2k-1} \\
& -c_1 \frac{n_{b_{k-1}}^3}{3} - \dots - c_{k-1} \frac{n_{b_1}^{2k-1}}{2k-1}
\end{aligned} \right] \quad (20)
\end{aligned}$$

and

$$\begin{aligned}
n_{b_k} = & \frac{1}{b_0} \left[(v_1 \mu^2 + \dots + v_k \mu^{2k}) - X_1 (u_1 \mu^2 + \dots + u_k \mu^{2k}) \right. \\
& - b_1 \frac{n_{b_{k-1}}^3}{3} - b_2 \frac{n_{b_{k-2}}^5}{5} - \dots - b_{k-1} \frac{n_{b_1}^{2k-1}}{2k-1} \\
& \left. - d_1 \frac{m_{a_{k-1}}^3}{3} - \dots - d_{k-1} \frac{m_{a_1}^{2k-1}}{2k-1} \right] \quad (21)
\end{aligned}$$

where m_{a_k} and n_{b_k} are defined by

$$m_a = m_{a_k} + \mathcal{O}(\mu^{2k+1}) \quad \text{and} \quad n_b = n_{b_k} + \mathcal{O}(\mu^{2k+1}) \quad (22)$$

and u_j as well as v_j are defined below in eq. (25).

It proves useful to augment the collection of integrals u and v by defining a third integral

$$w = \int_{-i}^i \frac{HX^2 dX}{W}. \quad (23)$$

Upon introducing the oblate spheroidal coordinates ξ and η

$$\rho = \rho_0 \sqrt{(1 + \xi^2)(1 - \eta^2)}, \quad \zeta = \rho_0 \xi \eta, \quad 0 \leq \xi < \infty, \quad -1 \leq \eta \leq 1 \quad (24)$$

one can come up with very simple, closed-form expressions for an arbitrary term in the series expansions of u , v and w about the point $\mu = 0$

$$u = \sum_{j=1}^{\infty} u_j \mu^{2j}, \quad v = \sum_{j=1}^{\infty} v_j \mu^{2j} \quad \text{and} \quad w = \sum_{j=1}^{\infty} w_j \mu^{2j}. \quad (25)$$

These expressions are given by

$$u_j = \alpha_{j-1} \int_0^{\text{arccot}(\xi)} \beta^{2j-1} dg \quad (26)$$

$$v_j = -\xi \eta \alpha_{j-1} \int_0^{\text{arccot}(\xi)} \tan^2(g) \beta^{2j-1} dg \quad (27)$$

$$w_j = \alpha_{j-1} \int_0^{\text{arccot}(\xi)} \gamma \beta^{2j-1} dg \quad (28)$$

$$\text{with } \beta = 1 - (1 + \xi^2)(1 - \eta^2) \sin^2(g) - \xi^2 \eta^2 \tan^2(g), \quad (29)$$

$$\gamma = -(1 + \xi^2)(1 - \eta^2) \sin^2(g) - \xi^2 \eta^2 \tan^2(g) \quad (30)$$

$$\text{and } \alpha_j = \frac{(-2)^{j+1} j!}{\pi(2j+1)!!}. \quad (31)$$

An expansion of the integrals I_1 and I_2 yields an expression in terms of m_{a_k} and n_{b_k} .⁴ These can in turn be expressed as a series in μ by expanding the coefficients a_i , b_i , c_i and d_i about the point $\mu = 0$. The integral I_3 , which can be written in the form

$$I_3 = w - (X_1 + X_2)v + X_1 X_2 u, \quad (32)$$

can easily be converted into a power series in μ by expanding X_1 and X_2 about the point $\mu = 0$. Thus a means of determining the coefficients f_n of eq. (14) and representing them in terms of u_j , v_j and w_j has been found.

4 Results

4.1 The Ernst Potential

The first eight coefficients in the expansion of the Ernst Potential are

$$f_1 = u_1, \quad (33)$$

$$f_2 = -i\sqrt{2}v_1, \quad (34)$$

$$f_3 = \frac{1}{2}u_1^2 - w_1, \quad (35)$$

$$f_4 = -i\left[\sqrt{2}u_1v_1 + \frac{1}{\sqrt{2}}v_1\right], \quad (36)$$

$$f_5 = u_2 + \frac{1}{2}u_1 + \frac{1}{6}u_1^3 - u_1w_1 - v_1^2, \quad (37)$$

$$f_6 = \frac{i\sqrt{2}}{24}\left[-3v_1 - 24v_2 + 8\xi\eta u_1^3 - 24u_1^2v_1 - 12u_1v_1 + 24v_1w_1\right], \quad (38)$$

$$f_7 = -w_2 - v_1^2 + \frac{1}{2}w_1^2 + \frac{1}{24}u_1^4 - \frac{1}{2}w_1u_1^2 - 2u_1v_1^2 + \frac{1}{2}u_1^2 + \frac{1}{3}u_1^3 - \frac{1}{3}u_1^3\eta^2 + \frac{1}{3}u_1^3\xi^2 + u_1u_2 \quad (39)$$

and

⁴One should be careful to choose the same sign for square roots in I_1 and I_2 as were chosen upon expanding eqs. (11) and (12).

$$\begin{aligned}
f_8 = & -\frac{i\sqrt{2}}{48} \left[-24 v_1^3 - 3 v_1 + 24 v_2 - 8 \xi \eta u_1^3 + 48 u_1^2 v_1 \right. \\
& + 30 u_1 v_1 - 24 v_1 w_1 - 48 \eta \xi u_1 v_1^2 - 24 \eta^2 u_1^2 v_1 \\
& + 24 \xi^2 u_1^2 v_1 + 48 v_1 u_2 + 32 u_1^3 v_1 - 16 u_1^4 \xi \eta \\
& \left. - 48 w_1 u_1 v_1 + 48 u_1 v_2 \right]. \tag{40}
\end{aligned}$$

Because u_j , v_j and w_j are all real quantities, one can see immediately that the coefficients f_n are alternately real and imaginary. Since the relativistic parameter is proportional to $1/c^2$, this series clearly exhibits the structure of the PN approximation, in which terms occur in pairs, the first of which is imaginary and of the order $\mathcal{O}(1/c^{2m-1})$, $m \in \mathbb{N}$, and the second of which is real and of the order $\mathcal{O}(1/c^{2m})$. Note that f_1 represents the Newtonian limit, i.e. the first truly post-Newtonian contribution is given by $m = 2$. Although the use of the expressions u_j , v_j and w_j provides a fairly succinct notation for the f_n , the coefficients still quickly become unwieldy with increasing n . For example, the expression for f_{24} would fill approximately 30 pages.

When the full expressions for u_1 , v_1 , w_1 and w_2 are substituted into eqs. (33), (35), (37) and (39), one obtains, using the abbreviation $\text{arccot}(\xi) = \chi$, the first four coefficients in the expansion of e^{2U} , $e^{2U} = 1 + \sum_{n=1}^{\infty} f_{2n-1} \mu^n$,

$$f_1 = -\frac{1}{\pi} \left[(3 \xi^2 \chi - 3 \xi + \chi) \eta^2 - \xi^2 \chi + \xi + \chi \right], \tag{41}$$

$$\begin{aligned}
f_3 = & \frac{1}{12\pi^2} \left[(54 \xi^4 \chi^2 + 105 \pi \xi^4 \chi - 108 \xi^3 \chi + 36 \xi^2 \chi^2 - 105 \pi \xi^3 + 90 \pi \xi^2 \chi \right. \\
& + 54 \xi^2 - 36 \xi \chi + 6 \chi^2 - 55 \pi \xi + 9 \pi \chi) \eta^4 + (-36 \xi^4 \chi^2 \\
& - 90 \pi \xi^4 \chi + 72 \xi^3 \chi + 24 \xi^2 \chi^2 + 90 \pi \xi^3 - 72 \pi \xi^2 \chi - 36 \xi^2 - 24 \xi \chi \\
& + 12 \chi^2 + 42 \pi \xi - 6 \pi \chi) \eta^2 + 6 \xi^4 \chi^2 + 9 \pi \xi^4 \chi - 12 \xi^3 \chi \\
& \left. - 12 \xi^2 \chi^2 - 9 \pi \xi^3 + 6 \pi \xi^2 \chi + 6 \xi^2 + 12 \xi \chi + 6 \chi^2 - 3 \pi \xi - 3 \pi \chi \right], \tag{42}
\end{aligned}$$

$$\begin{aligned}
f_5 = & -\frac{1}{180\pi^3} \left[(810 \xi^6 \chi^3 + 9225 \pi \xi^6 \chi^2 - 3465 \pi^2 \xi^6 \chi - 2430 \xi^5 \chi^2 + 810 \xi^4 \chi^3 \right. \\
& - 18450 \pi \xi^5 \chi + 11025 \pi \xi^4 \chi^2 + 3465 \pi^2 \xi^5 + 2430 \xi^4 \chi - 4725 \pi^2 \xi^4 \chi \\
& - 1620 \xi^3 \chi^2 + 270 \xi^2 \chi^3 + 9225 \pi \xi^4 - 15900 \pi \xi^3 \chi + 3375 \pi \xi^2 \chi^2 \\
& - 810 \xi^3 + 3570 \pi^2 \xi^3 - 1575 \pi^2 \xi^2 \chi + 810 \xi^2 \chi - 270 \xi \chi^2 + 30 \chi^3 \\
& + 4875 \pi \xi^2 - 2670 \pi \xi \chi + 135 \pi \chi^2 + 693 \pi^2 \xi - 75 \pi^2 \chi + 320 \pi) \eta^6 \\
& + (-810 \xi^6 \chi^3 - 11025 \pi \xi^6 \chi^2 + 4725 \pi^2 \xi^6 \chi + 2430 \xi^5 \chi^2 \\
& + 270 \xi^4 \chi^3 + 22050 \pi \xi^5 \chi - 9405 \pi \xi^4 \chi^2 - 4725 \pi^2 \xi^5 - 2430 \xi^4 \chi \\
& + 4725 \pi^2 \xi^4 \chi - 540 \xi^3 \chi^2 + 450 \xi^2 \chi^3 - 11025 \pi \xi^4 + 13560 \pi \xi^3 \chi \\
& - 1215 \pi \xi^2 \chi^2 + 810 \xi^3 - 3150 \pi^2 \xi^3 + 675 \pi^2 \xi^2 \chi + 270 \xi^2 \chi - 450 \xi \chi^2 \\
& + 90 \chi^3 - 4155 \pi \xi^2 + 690 \pi \xi \chi + 45 \pi \chi^2 - 45 \pi^2 \xi - 45 \pi^2 \chi) \eta^4 \\
& + (270 \xi^6 \chi^3 + 3375 \pi \xi^6 \chi^2 - 1575 \pi^2 \xi^6 \chi - 810 \xi^5 \chi^2 - 450 \xi^4 \chi^3 \\
& \left. - 6750 \pi \xi^5 \chi + 1215 \pi \xi^4 \chi^2 + 1575 \pi^2 \xi^5 + 810 \xi^4 \chi - 675 \pi^2 \xi^4 \chi \right]
\end{aligned}$$

$$\begin{aligned}
& + 900 \xi^3 \chi^2 + 90 \xi^2 \chi^3 + 3375 \pi \xi^4 - 1980 \pi \xi^3 \chi - 855 \pi \xi^2 \chi^2 - 270 \xi^3 \\
& + 150 \pi^2 \xi^3 + 405 \pi^2 \xi^2 \chi - 450 \xi^2 \chi - 90 \xi \chi^2 + 90 \chi^3 + 765 \pi \xi^2 \\
& + 630 \pi \xi \chi - 135 \pi \chi^2 - 315 \pi^2 \xi + 45 \pi^2 \chi) \eta^2 - 30 \xi^6 \chi^3 \\
& - 135 \pi \xi^6 \chi^2 + 75 \pi^2 \xi^6 \chi + 90 \xi^5 \chi^2 + 90 \xi^4 \chi^3 + 270 \pi \xi^5 \chi + 45 \pi \xi^4 \chi^2 \\
& - 75 \pi^2 \xi^5 - 90 \xi^4 \chi - 45 \pi^2 \xi^4 \chi - 180 \xi^3 \chi^2 - 90 \xi^2 \chi^3 - 135 \pi \xi^4 \\
& + 135 \pi \xi^2 \chi^2 + 30 \xi^3 + 70 \pi^2 \xi^3 - 45 \pi^2 \xi^2 \chi + 90 \xi^2 \chi + 90 \xi \chi^2 + 30 \chi^3 \\
& - 45 \pi \xi^2 - 90 \pi \xi \chi - 45 \pi \chi^2 + 15 \pi^2 \xi + 15 \pi^2 \chi] \quad (43)
\end{aligned}$$

and

$$\begin{aligned}
f_7 = & \frac{1}{10080\pi^4} \left[(34020 \xi^8 \chi^4 + 1908900 \pi \xi^8 \chi^3 - 196245 \pi^2 \xi^8 \chi^2 - 136080 \xi^7 \chi^3 \right. \\
& + 45360 \xi^6 \chi^4 - 675675 \pi^3 \xi^8 \chi - 5726700 \pi \xi^7 \chi^2 + 3013920 \pi \xi^6 \chi^3 \\
& + 392490 \pi^2 \xi^7 \chi - 326340 \pi^2 \xi^6 \chi^2 + 204120 \xi^6 \chi^2 - 136080 \xi^5 \chi^3 \\
& + 22680 \xi^4 \chi^4 + 675675 \pi^3 \xi^7 + 5726700 \pi \xi^6 \chi - 1261260 \pi^3 \xi^6 \chi \\
& - 7132860 \pi \xi^5 \chi^2 + 1544760 \pi \xi^4 \chi^3 - 196245 \pi^2 \xi^6 + 521850 \pi^2 \xi^5 \chi \\
& - 136080 \xi^5 \chi + 136080 \xi^4 \chi^2 - 179550 \pi^2 \xi^4 \chi^2 - 45360 \xi^3 \chi^3 \\
& + 5040 \xi^2 \chi^4 + 1036035 \pi^3 \xi^5 - 1908900 \pi \xi^5 - 727650 \pi^3 \xi^4 \chi \\
& + 5223960 \pi \xi^4 \chi - 2560740 \pi \xi^3 \chi^2 + 272160 \pi \xi^2 \chi^3 + 34020 \xi^4 \\
& - 195510 \pi^2 \xi^4 - 45360 \xi^3 \chi + 168294 \pi^2 \xi^3 \chi + 22680 \xi^2 \chi^2 \\
& - 44100 \pi^2 \xi^2 \chi^2 - 5040 \xi \chi^3 + 420 \chi^4 + 442365 \pi^3 \xi^3 - 1105020 \pi \xi^3 \\
& - 132300 \pi^3 \xi^2 \chi + 1123500 \pi \xi^2 \chi - 237300 \pi \xi \chi^2 + 7140 \pi \chi^3 \\
& - 10549 \pi^2 \xi^2 + 16758 \pi^2 \xi \chi - 1365 \pi^2 \chi^2 + 45477 \pi^3 \xi - 107520 \pi \xi \\
& + 35840 \pi \chi - 3675 \pi^3 \chi) \eta^8 + (-45360 \xi^8 \chi^4 \\
& - 3013920 \pi \xi^8 \chi^3 + 326340 \pi^2 \xi^8 \chi^2 + 181440 \xi^7 \chi^3 + 1261260 \pi^3 \xi^8 \chi \\
& + 9041760 \pi \xi^7 \chi^2 - 3220560 \pi \xi^6 \chi^3 - 652680 \pi^2 \xi^7 \chi - 219240 \pi^2 \xi^6 \chi^2 \\
& - 272160 \xi^6 \chi^2 + 30240 \xi^4 \chi^4 - 1261260 \pi^3 \xi^7 + 2134440 \pi^3 \xi^6 \chi \\
& - 9041760 \pi \xi^6 \chi + 7672560 \pi \xi^5 \chi^2 - 619920 \pi \xi^4 \chi^3 + 326340 \pi^2 \xi^6 \\
& + 181440 \xi^5 \chi + 397320 \pi^2 \xi^5 \chi - 655200 \pi^2 \xi^4 \chi^2 - 60480 \xi^3 \chi^3 \\
& + 13440 \xi^2 \chi^4 + 3013920 \pi \xi^5 - 1714020 \pi^3 \xi^5 + 1058400 \pi^3 \xi^4 \chi \\
& - 5683440 \pi \xi^4 \chi + 954240 \pi \xi^3 \chi^2 + 122640 \pi \xi^2 \chi^3 - 178080 \pi^2 \xi^4 \\
& - 45360 \xi^4 + 854952 \pi^2 \xi^3 \chi - 227640 \pi^2 \xi^2 \chi^2 + 30240 \xi^2 \chi^2 \\
& - 13440 \xi \chi^3 + 1680 \chi^4 - 599172 \pi^3 \xi^3 + 1231440 \pi \xi^3 - 370160 \pi \xi^2 \chi \\
& + 147000 \pi^3 \xi^2 \chi - 156240 \pi \xi \chi^2 + 11760 \pi \chi^3 - 249732 \pi^2 \xi^2 \\
& + 169848 \pi^2 \xi \chi - 10500 \pi^2 \chi^2 - 40908 \pi^3 \xi + 35840 \pi \xi + 35840 \pi \chi \\
& + 2100 \pi^3 \chi - 17920 \pi^2) \eta^6 + (22680 \xi^8 \chi^4 + 1544760 \pi \xi^8 \chi^3 \\
& - 179550 \pi^2 \xi^8 \chi^2 - 90720 \xi^7 \chi^3 - 30240 \xi^6 \chi^4 - 727650 \pi^3 \xi^8 \chi \\
& - 4634280 \pi \xi^7 \chi^2 + 619920 \pi \xi^6 \chi^3 + 359100 \pi^2 \xi^7 \chi + 136080 \xi^6 \chi^2 \\
& + 655200 \pi^2 \xi^6 \chi^2 + 90720 \xi^5 \chi^3 - 5040 \xi^4 \chi^4 + 727650 \pi^3 \xi^7
\end{aligned}$$

$$\begin{aligned}
& + 4634280 \pi \xi^6 \chi - 1058400 \pi^3 \xi^6 \chi - 1662360 \pi \xi^5 \chi^2 - 594720 \pi \xi^4 \chi^3 \\
& - 179550 \pi^2 \xi^6 - 1077300 \pi^2 \xi^5 \chi - 90720 \xi^5 \chi - 90720 \xi^4 \chi^2 \\
& + 779940 \pi^2 \xi^4 \chi^2 + 10080 \xi^3 \chi^3 + 10080 \xi^2 \chi^4 + 815850 \pi^3 \xi^5 \\
& - 1544760 \pi \xi^5 - 396900 \pi^3 \xi^4 \chi + 1464960 \pi \xi^4 \chi + 884520 \pi \xi^3 \chi^2 \\
& - 196560 \pi \xi^2 \chi^3 + 422100 \pi^2 \xi^4 + 22680 \xi^4 + 30240 \xi^3 \chi \\
& - 886620 \pi^2 \xi^3 \chi + 146160 \pi^2 \xi^2 \chi^2 - 5040 \xi^2 \chi^2 - 10080 \xi \chi^3 + 2520 \chi^4 \\
& + 189630 \pi^3 \xi^3 - 422520 \pi \xi^3 - 25200 \pi^3 \xi^2 \chi - 289800 \pi \xi^2 \chi \\
& + 130200 \pi \xi \chi^2 - 2520 \pi \chi^3 + 204330 \pi^2 \xi^2 - 65100 \pi^2 \xi \chi - 630 \pi^2 \chi^2 \\
& + 630 \pi^3 \xi + 630 \pi^3 \chi) \eta^4 + (-5040 \xi^8 \chi^4 - 272160 \pi \xi^8 \chi^3 \\
& + 44100 \pi^2 \xi^8 \chi^2 + 20160 \xi^7 \chi^3 + 13440 \xi^6 \chi^4 + 132300 \pi^3 \xi^8 \chi \\
& + 816480 \pi \xi^7 \chi^2 + 122640 \pi \xi^6 \chi^3 - 88200 \pi^2 \xi^7 \chi - 227640 \pi^2 \xi^6 \chi^2 \\
& - 30240 \xi^6 \chi^2 - 40320 \xi^5 \chi^3 - 10080 \xi^4 \chi^4 - 132300 \pi^3 \xi^7 \\
& + 147000 \pi^3 \xi^6 \chi - 816480 \pi \xi^6 \chi - 186480 \pi \xi^5 \chi^2 + 196560 \pi \xi^4 \chi^3 \\
& + 44100 \pi^2 \xi^6 + 20160 \xi^5 \chi + 367080 \pi^2 \xi^5 \chi - 146160 \pi^2 \xi^4 \chi^2 \\
& + 40320 \xi^4 \chi^2 + 20160 \xi^3 \chi^3 + 272160 \pi \xi^5 - 102900 \pi^3 \xi^5 + 5040 \pi \xi^4 \chi \\
& + 25200 \pi^3 \xi^4 \chi - 302400 \pi \xi^3 \chi^2 - 35280 \pi \xi^2 \chi^3 - 139440 \pi^2 \xi^4 \\
& - 5040 \xi^4 - 13440 \xi^3 \chi + 140840 \pi^2 \xi^3 \chi - 10080 \xi^2 \chi^2 + 22680 \pi^2 \xi^2 \chi^2 \\
& + 1680 \chi^4 - 2660 \pi^3 \xi^3 + 58800 \pi \xi^3 + 105840 \pi \xi^2 \chi - 2520 \pi^3 \xi^2 \chi \\
& + 35280 \pi \xi \chi^2 - 11760 \pi \chi^3 - 28980 \pi^2 \xi^2 - 24360 \pi^2 \xi \chi + 4620 \pi^2 \chi^2 \\
& + 420 \pi^3 \xi + 420 \pi^3 \chi) \eta^2 + 420 \xi^8 \chi^4 + 7140 \pi \xi^8 \chi^3 \\
& - 1365 \pi^2 \xi^8 \chi^2 - 1680 \xi^7 \chi^3 - 1680 \xi^6 \chi^4 - 3675 \pi^3 \xi^8 \chi - 21420 \pi \xi^7 \chi^2 \\
& - 11760 \pi \xi^6 \chi^3 + 2730 \pi^2 \xi^7 \chi + 2520 \xi^6 \chi^2 + 10500 \pi^2 \xi^6 \chi^2 \\
& + 5040 \xi^5 \chi^3 + 2520 \xi^4 \chi^4 + 3675 \pi^3 \xi^7 + 21420 \pi \xi^6 \chi - 2100 \pi^3 \xi^6 \chi \\
& + 18900 \pi \xi^5 \chi^2 - 2520 \pi \xi^4 \chi^3 - 1365 \pi^2 \xi^6 - 16310 \pi^2 \xi^5 \chi - 1680 \xi^5 \chi \\
& - 5040 \xi^4 \chi^2 - 630 \pi^2 \xi^4 \chi^2 - 5040 \xi^3 \chi^3 - 1680 \xi^2 \chi^4 + 875 \pi^3 \xi^5 \\
& - 7140 \pi \xi^5 + 630 \pi^3 \xi^4 \chi - 2520 \pi \xi^4 \chi + 16380 \pi \xi^3 \chi^2 + 11760 \pi \xi^2 \chi^3 \\
& + 5810 \pi^2 \xi^4 + 420 \xi^4 + 1680 \xi^3 \chi + 1190 \pi^2 \xi^3 \chi - 4620 \pi^2 \xi^2 \chi^2 \\
& + 2520 \xi^2 \chi^2 + 1680 \xi \chi^3 + 420 \chi^4 - 595 \pi^3 \xi^3 - 4620 \pi \xi^3 - 420 \pi^3 \xi^2 \chi \\
& - 13860 \pi \xi^2 \chi - 13860 \pi \xi \chi^2 - 4620 \pi \chi^3 + 1155 \pi^2 \xi^2 + 2310 \pi^2 \xi \chi \\
& + 1155 \pi^2 \chi^2 + 525 \pi^3 \xi + 525 \pi^3 \chi \Big]. \tag{44}
\end{aligned}$$

Calculating the appropriate line integrals, one can determine the remaining metric functions a and k . Using the expansions

$$a = \sum_{n=1}^{\infty} a_{2n} \mu^{(2n+1)/2} \quad \text{and} \quad e^{2k} = 1 + \sum_{n=1}^{\infty} K_{2n-1} \mu^n, \tag{45}$$

one finds the expressions

$$a_2 = \frac{\sqrt{2}\rho_0}{4\pi} [1 - \eta^2] \left[(15\xi^4\chi - 15\xi^3 + 18\xi^2\chi - 13\xi + 3\chi)\eta^2 - 3\xi^4\chi + 3\xi^3 - 2\xi^2\chi + \xi + \chi \right], \quad (46)$$

$$a_4 = \frac{\sqrt{2}\rho_0}{72\pi^2} [1 - \eta^2] \left[(180\xi^6\chi^2 - 360\xi^5\chi + 252\xi^4\chi^2 + 180\xi^4 - 384\xi^3\chi + 108\xi^2\chi^2 + 132\xi^2 - 24\xi\chi + 36\chi^2 - 64)\eta^4 + (-72\xi^6\chi^2 + 144\xi^5\chi + 216\xi^4\chi^2 + 135\pi\xi^4\chi - 72\xi^4 + 360\xi^2\chi^2 - 135\pi\xi^3 + 162\pi\xi^2\chi - 216\xi^2 - 144\xi\chi + 72\chi^2 - 117\pi\xi + 27\pi\chi - 64)\eta^2 + 36\xi^6\chi^2 - 72\xi^5\chi - 36\xi^4\chi^2 - 27\pi\xi^4\chi + 36\xi^4 - 36\xi^2\chi^2 + 27\pi\xi^3 - 18\pi\xi^2\chi + 36\xi^2 + 72\xi\chi + 36\chi^2 + 9\pi\xi + 9\pi\chi - 64 \right], \quad (47)$$

$$a_6 = \frac{\sqrt{2}\rho_0}{1440\pi^3} [1 - \eta^2] \left[(12960\xi^8\chi^3 + 7875\pi\xi^8\chi^2 - 45045\pi^2\xi^8\chi - 38880\xi^7\chi^2 + 25920\xi^6\chi^3 - 15750\pi\xi^7\chi + 15300\pi\xi^6\chi^2 + 45045\pi^2\xi^7 - 38880\xi^6\chi - 97020\pi^2\xi^6\chi - 64800\xi^5\chi^2 + 17280\xi^4\chi^3 + 7875\pi\xi^6 - 25350\pi\xi^5\chi + 9450\pi\xi^4\chi^2 - 12960\xi^5 + 82005\pi^2\xi^5 + 51840\xi^4\chi - 66150\pi^2\xi^4\chi - 30240\xi^3\chi^2 + 4800\xi^2\chi^3 + 10050\pi\xi^4 - 11850\pi\xi^3\chi + 1620\pi\xi^2\chi^2 - 12960\xi^3 + 42819\pi^2\xi^3 + 12960\xi^2\chi - 14700\pi^2\xi^2\chi - 4320\xi\chi^2 + 480\chi^3 + 3275\pi\xi^2 - 2250\pi\xi\chi - 405\pi\chi^2 + 5619\pi^2\xi - 525\pi^2\chi + 1280\pi)\eta^6 + (-12960\xi^8\chi^3 - 7425\pi\xi^8\chi^2 + 51975\pi^2\xi^8\chi + 38880\xi^7\chi^2 - 8640\xi^6\chi^3 + 14850\pi\xi^7\chi - 8100\pi\xi^6\chi^2 - 51975\pi^2\xi^7 - 38880\xi^6\chi + 94500\pi^2\xi^6\chi + 30240\xi^5\chi^2 + 11520\xi^4\chi^3 - 7425\pi\xi^6 + 11250\pi\xi^5\chi - 630\pi\xi^4\chi^2 + 12960\xi^5 - 77175\pi^2\xi^5 - 34560\xi^4\chi + 47250\pi^2\xi^4\chi - 15840\xi^3\chi^2 + 8640\xi^2\chi^3 - 3150\pi\xi^4 - 4530\pi\xi^3\chi + 540\pi\xi^2\chi^2 + 12960\xi^3 - 26145\pi^2\xi^3 + 4320\xi^2\chi + 4500\pi^2\xi^2\chi - 7200\xi\chi^2 + 1440\chi^3 + 4335\pi\xi^2 - 930\pi\xi\chi + 495\pi\chi^2 - 225\pi^2\xi - 225\pi^2\chi - 640\pi)\eta^4 + (4320\xi^8\chi^3 + 2025\pi\xi^8\chi^2 - 14175\pi^2\xi^8\chi - 12960\xi^7\chi^2 - 2880\xi^6\chi^3 - 4050\pi\xi^7\chi + 1980\pi\xi^6\chi^2 + 14175\pi^2\xi^7 + 12960\xi^6\chi - 18900\pi^2\xi^6\chi + 1440\xi^5\chi^2 - 5760\xi^4\chi^3 + 2025\pi\xi^6 - 2610\pi\xi^5\chi + 4590\pi\xi^4\chi^2 + 14175\pi^2\xi^5 - 4320\xi^5 - 3375\pi^2\xi^4\chi + 5760\xi^4\chi + 12960\xi^3\chi^2 + 2880\xi^2\chi^3 + 630\pi\xi^4 - 990\pi\xi^3\chi + 5580\pi\xi^2\chi^2 - 4320\xi^3 - 90\pi^2\xi^3 + 1350\pi^2\xi^2\chi - 7200\xi^2\chi - 1440\xi\chi^2 + 1440\chi^3 - 3375\pi\xi^2 - 2430\pi\xi\chi + 945\pi\chi^2 - 720\pi^2\xi - 640\pi)\eta^2 - 480\xi^8\chi^3 + 405\pi\xi^8\chi^2 + 525\pi^2\xi^8\chi + 1440\xi^7\chi^2 + 960\xi^6\chi^3 - 810\pi\xi^7\chi + 900\pi\xi^6\chi^2 - 525\pi^2\xi^7 - 1440\xi^6\chi + 300\pi^2\xi^6\chi \right]$$

$$\begin{aligned}
& -1440 \xi^5 \chi^2 + 405 \pi \xi^6 - 1530 \pi \xi^5 \chi - 450 \pi \xi^4 \chi^2 - 125 \pi^2 \xi^5 + 480 \xi^5 \\
& - 225 \pi^2 \xi^4 \chi - 1440 \xi^3 \chi^2 - 960 \xi^2 \chi^3 + 630 \pi \xi^4 + 90 \pi \xi^3 \chi \\
& - 540 \pi \xi^2 \chi^2 + 220 \pi^2 \xi^3 + 480 \xi^3 + 1440 \xi^2 \chi - 30 \pi^2 \xi^2 \chi + 1440 \xi \chi^2 \\
& + 480 \chi^3 + 405 \pi \xi^2 + 810 \pi \xi \chi + 405 \pi \chi^2 - 30 \pi^2 \xi - 30 \pi^2 \chi - 640 \pi \Big], \quad (48)
\end{aligned}$$

$$K_1 = 0, \quad (49)$$

$$\begin{aligned}
K_3 = & -\frac{1}{2\pi^2} \left[1 - \eta^2 \right] \left[(9 \xi^4 \chi^2 - 18 \xi^3 \chi + 10 \xi^2 \chi^2 + 9 \xi^2 - 14 \xi \chi + \chi^2 + 4) \eta^2 \right. \\
& \left. - \xi^4 \chi^2 + 2 \xi^3 \chi - 2 \xi^2 \chi^2 - \xi^2 - 2 \xi \chi - \chi^2 + 4 \right], \quad (50)
\end{aligned}$$

$$\begin{aligned}
K_5 = & -\frac{1}{18\pi^2} \left[1 - \eta^2 \right] \left[(45 \xi^6 \chi^2 - 90 \xi^5 \chi + 63 \xi^4 \chi^2 + 45 \xi^4 - 96 \xi^3 \chi + 27 \xi^2 \chi^2 \right. \\
& + 33 \xi^2 - 6 \xi \chi + 9 \chi^2 - 16) \eta^4 + (-18 \xi^6 \chi^2 + 36 \xi^5 \chi + 54 \xi^4 \chi^2 - 18 \xi^4 \\
& + 90 \xi^2 \chi^2 - 54 \xi^2 - 36 \xi \chi + 18 \chi^2 - 16) \eta^2 \\
& \left. + 9 \xi^6 \chi^2 - 18 \xi^5 \chi - 9 \xi^4 \chi^2 + 9 \xi^4 - 9 \xi^2 \chi^2 + 9 \xi^2 + 18 \xi \chi + 9 \chi^2 - 16 \right] \quad (51)
\end{aligned}$$

and

$$\begin{aligned}
K_7 = & -\frac{1}{720\pi^4} \left[1 - \eta^2 \right] \left[(7290 \xi^8 \chi^4 - 7245 \pi^2 \xi^8 \chi^2 - 29160 \xi^7 \chi^3 + 16200 \xi^6 \chi^4 \right. \\
& + 14490 \pi^2 \xi^7 \chi - 16020 \pi^2 \xi^6 \chi^2 + 43740 \xi^6 \chi^2 - 55080 \xi^5 \chi^3 \\
& + 10620 \xi^4 \chi^4 - 7245 \pi^2 \xi^6 + 27210 \pi^2 \xi^5 \chi - 29160 \xi^5 \chi - 10350 \pi^2 \xi^4 \chi^2 \\
& + 68040 \xi^4 \chi^2 - 28440 \xi^3 \chi^3 + 1800 \xi^2 \chi^4 + 7290 \xi^4 - 11190 \pi^2 \xi^4 \\
& + 14934 \pi^2 \xi^3 \chi - 35640 \xi^3 \chi - 1620 \pi^2 \xi^2 \chi^2 + 26460 \xi^2 \chi^2 - 2520 \xi \chi^3 \\
& + 90 \chi^4 + 6480 \xi^2 - 5389 \pi^2 \xi^2 + 1734 \pi^2 \xi \chi - 10080 \xi \chi - 45 \pi^2 \chi^2 \\
& + 720 \chi^2 - 256 \pi^2 + 1440) \eta^6 + (-8910 \xi^8 \chi^4 + 8775 \pi^2 \xi^8 \chi^2 \\
& + 35640 \xi^7 \chi^3 - 21240 \xi^6 \chi^4 - 17550 \pi^2 \xi^7 \chi + 22500 \pi^2 \xi^6 \chi^2 \\
& - 53460 \xi^6 \chi^2 + 64440 \xi^5 \chi^3 - 16020 \xi^4 \chi^4 + 8775 \pi^2 \xi^6 - 29070 \pi^2 \xi^5 \chi \\
& + 35640 \xi^5 \chi + 17730 \pi^2 \xi^4 \chi^2 - 65880 \xi^4 \chi^2 + 33480 \xi^3 \chi^3 - 3960 \xi^2 \chi^4 \\
& - 8910 \xi^4 + 6570 \pi^2 \xi^4 - 13890 \pi^2 \xi^3 \chi + 23400 \xi^3 \chi + 4500 \pi^2 \xi^2 \chi^2 \\
& - 17460 \xi^2 \chi^2 + 4680 \xi \chi^3 - 270 \chi^4 - 720 \xi^2 + 495 \pi^2 \xi^2 - 930 \pi^2 \xi \chi \\
& - 1440 \xi \chi + 495 \pi^2 \chi^2 - 720 \chi^2 - 896 \pi^2 + 1440) \eta^4 \\
& + (1710 \xi^8 \chi^4 - 1575 \pi^2 \xi^8 \chi^2 - 6840 \xi^7 \chi^3 + 5400 \xi^6 \chi^4 + 3150 \pi^2 \xi^7 \chi \\
& + 10260 \xi^6 \chi^2 - 5580 \pi^2 \xi^6 \chi^2 - 9720 \xi^5 \chi^3 + 5940 \xi^4 \chi^4 - 1575 \pi^2 \xi^6 \\
& + 3390 \pi^2 \xi^5 \chi - 6840 \xi^5 \chi - 3240 \xi^4 \chi^2 - 2970 \pi^2 \xi^4 \chi^2 - 4680 \xi^3 \chi^3 \\
& + 2520 \xi^2 \chi^4 + 1710 \xi^4 + 2190 \pi^2 \xi^4 + 14040 \xi^3 \chi + 1410 \pi^2 \xi^3 \chi \\
& + 1620 \pi^2 \xi^2 \chi^2 - 9900 \xi^2 \chi^2 - 1800 \xi \chi^3 + 270 \chi^4 - 6480 \xi^2 - 855 \pi^2 \xi^2 \\
& + 10080 \xi \chi - 270 \pi^2 \xi \chi + 585 \pi^2 \chi^2 - 720 \chi^2 - 1440 - 896 \pi^2) \eta^2 \\
& - 90 \xi^8 \chi^4 + 45 \pi^2 \xi^8 \chi^2 + 360 \xi^7 \chi^3 - 360 \xi^6 \chi^4 - 90 \pi^2 \xi^7 \chi \\
& \left. - 540 \xi^6 \chi^2 + 540 \pi^2 \xi^6 \chi^2 + 360 \xi^5 \chi^3 - 540 \xi^4 \chi^4 + 45 \pi^2 \xi^6 - 570 \pi^2 \xi^5 \chi \right]
\end{aligned}$$

$$\begin{aligned}
& + 360 \xi^5 \chi + 1080 \xi^4 \chi^2 - 90 \pi^2 \xi^4 \chi^2 - 360 \xi^3 \chi^3 - 360 \xi^2 \chi^4 - 90 \xi^4 \\
& + 30 \pi^2 \xi^4 - 1800 \xi^3 \chi - 150 \pi^2 \xi^3 \chi - 180 \pi^2 \xi^2 \chi^2 + 900 \xi^2 \chi^2 - 360 \xi \chi^3 \\
& - 90 \chi^4 + 720 \xi^2 + 405 \pi^2 \xi^2 + 1440 \xi \chi + 810 \pi^2 \xi \chi + 405 \pi^2 \chi^2 + 720 \chi^2 \\
& - 1440 - 896 \pi^2 \Big]. \tag{52}
\end{aligned}$$

Eqs. (41)-(52) provide the full metric up to and including the order $\mathcal{O}(\mu^4)$.

Making use of the metric functions, one can furthermore find the series expansion for other quantities of interest:

$$e^{2V_0} = 1 - \mu + \frac{1}{2} \mu^2 - \frac{16}{9\pi^2} \mu^3 + \left(\frac{16}{9\pi^2} - \frac{1}{8} \right) \mu^4 + \mathcal{O}(\mu^5), \tag{53}$$

$$\begin{aligned}
\Omega\rho_0 &= \frac{\sqrt{2}}{2} \mu^{1/2} - \frac{\sqrt{2}}{4} \mu^{3/2} + \frac{\sqrt{2}}{16} \mu^{5/2} \\
&+ \frac{\sqrt{2}}{2} \left(-\frac{8}{9\pi^2} + \frac{1}{16} \right) \mu^{7/2} + \mathcal{O}(\mu^{9/2}) \tag{54}
\end{aligned}$$

and

$$\begin{aligned}
\sigma_P/\Omega &= \frac{\sqrt{2}\eta}{\pi^2} \mu^{1/2} + \left(-\frac{7\sqrt{2}\eta^3}{12\pi^2} + \frac{\sqrt{2}\eta}{4\pi^2} \right) \mu^{3/2} \\
&+ \left(\frac{163\sqrt{2}\eta^5}{480\pi^2} - \frac{7\sqrt{2}\eta^3}{48\pi^2} - \frac{3\sqrt{2}\eta}{32\pi^2} + \frac{\sqrt{2}\eta}{\pi^4} - \frac{\sqrt{2}\eta^5}{\pi^4} \right) \mu^{5/2} \\
&+ \left(-\frac{9\sqrt{2}\eta}{128\pi^2} + \frac{163\sqrt{2}\eta^5}{1920\pi^2} + \frac{7\sqrt{2}\eta^3}{128\pi^2} - \frac{59\eta^7\sqrt{2}}{36\pi^4} + \frac{1117\eta^7\sqrt{2}}{13440\pi^2} \right. \\
&\left. - \frac{7\eta^3\sqrt{2}}{12\pi^4} - \frac{\sqrt{2}\eta^5}{4\pi^4} + \frac{25\sqrt{2}\eta}{36\pi^4} \right) \mu^{7/2} + \mathcal{O}(\mu^{9/2}). \tag{55}
\end{aligned}$$

Related to the fact that the first four f_n can be calculated without making use of the Jacobi inversion problem, Bardeen and Wagoner were able to determine them in [4]. Taking into account that the relativistic parameter used in said paper is somewhat different,⁵ the coefficients calculated by Bardeen and Wagoner were compared with eqs. (33)-(36) and found to be in agreement. Using the knowledge that these first coefficients are correct, a further twelve f_n have been proved correct by showing that they satisfy the Ernst equation up to the relevant order. The further eight coefficients that were explicitly calculated could not undergo the same test due to computer limitations, but were calculated using the same iteration scheme, whence their correctness is all but certain. For more details see [6].

While a direct comparison of the PN expansion of the Ernst potential to the numerical results of Bardeen and Wagoner is not feasible for an arbitrary point in space, various quantities in the disc can be compared quite readily. In particular, the analytical version of Table 2 in [4] was drawn up, presenting

⁵Bardeen and Wagoner chose to use the relativistic parameter γ defined by $\gamma = 1 - e^{V_0}$. The series forms of the functions $\gamma = \gamma(\mu)$ and $\mu = \mu(\gamma)$ can be calculated using the function $V_0 = V_0(\mu)$ (see [2]) and are listed up to the orders $\mathcal{O}(\mu^{12})$ and $\mathcal{O}(\gamma^{12})$ respectively in [6].

the series for the square of the linear velocity, v^2 , for some particle of the disc as measured in the locally nonrotating frame of reference. It turns out that the numerical results, which are listed to the 5th decimal place, are perfectly correct up to the order $\mathcal{O}(\gamma^5)$.⁶ As to be expected, the expansion coefficients differ more and more from the analytic values as one moves to higher orders of the series. The last entry in Table 2 of [4] deviates from the analytic result by approximately 25%. In all however, the numerical results in Bardeen and Wagoner are highly accurate and seldom differ from the analytic ones by more than a fraction of a percent.

4.2 Convergence

As could have been expected right from the outset, the convergence of the PN approximation depends to a great extent on position, i.e. on the coordinates ξ and η . For example, on the rim of the disc itself, the Ernst potential is given by the analytic expression $f = 1 - \mu/2$, whereas in general, the potential is given by an infinite series in μ . Plots similar to that of Fig. 1 strongly indicate that the series converges for spatial infinity ($\xi \rightarrow \infty$) and has a radius of convergence of precisely μ_0 in this limit. Evaluations of the series at various (arbitrary) points in space indicate, moreover, that it converges everywhere. The series tends to converge quite quickly for small $|\eta|$, but rather erratically for $|\eta|$ nearing 1 ($\eta = \pm 1$ corresponds to the axis of symmetry).

The Padé approximant, which represents a truncated series via a rational polynomial expression, proves to be a highly advantageous alternative to the series, in particular if the original series converges slowly, erratically or not at all. Using this approximant, the erratic convergence of the PN expansion for the Ernst potential near the axis or the particularly slow convergence of the dimensionless quantity $\Omega\rho_0$ can be largely circumvented. Frequent use of the Padé approximant was made in the work of Bardeen and Wagoner [4]. In this paper however, sparing use of it is made so as better to concentrate on the PN expansion itself, but a comparison of the Padé approximant to the standard PN series can be found in Table 2. Let it be mentioned that the proper surface mass density (Fig. 2) and the ergospheres (Figs. 3 and 4) can be found to extremely high accuracy using the Padé approximant. A general discussion of the Padé approximant can be found in [7] and a consideration of its use in the PN expansion in [8].

In Figure 1, the ratio of consecutive coefficients from the real and imaginary parts of the Ernst potential has been plotted to illustrate the convergence of the series for a chosen point in space. In order to have a measure for the leading terms of the expansion, we took f_0 to be 1 and f_{-1} to be i . Note that the series is guaranteed to converge at a given value of μ , say $\mu = \mu_c$, so long as the condition $\lim_{n \rightarrow \infty} |f_{n+1}/f_{n-1}| < 1/\mu_c$ is met. Thus the series always converges in the Newtonian limit $\mu \rightarrow 0$ and converges in the limit $\mu \rightarrow \mu_0$ so long as $\lim_{n \rightarrow \infty} |f_{n+1}/f_{n-1}| < 1/\mu_0 \approx 0.21$ holds.

⁶The results concerning v^2 were calculated using the parameter γ in order to facilitate the

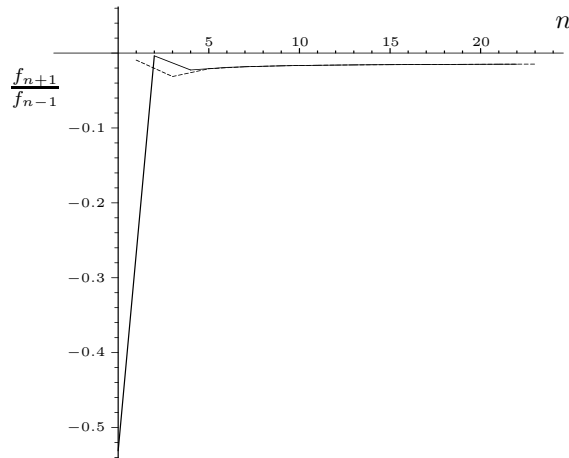


Figure 1: The ratio of consecutive real and imaginary coefficients from the expansion of f taken at a point $\xi = 0$, $\eta = 3/5$ in the disc. The solid line represents the real coefficients and the dotted line the imaginary coefficients.

In Fig. 1 one sees that the series converges quite quickly for this point on the disc, that f_1 plays a fairly important role, but that f_3 and higher coefficients contribute little to the potential. The fact that the ratio of consecutive coefficients of the series is negative means that these coefficients alternate sign, so that one always has an upper and lower bound on the value for (the real and imaginary parts of) f . Note that not all points in space exhibit such clear convergence as that of Fig. 1.

Not only does the applicability of the series depend upon the point in space that is chosen, but of course upon the value of μ as well. It goes without saying that the PN approximation reflects the full field equations fairly accurately for small values of μ , but we shall see further, as did Bardeen and Wagoner much to their surprise, that the approximation can be utilized to great benefit even in many highly relativistic situations. Looking at Table 1, one can see that the PN approximation of order $\mathcal{O}(\mu^{25/2})$ returns values for f that are correct to at least 9 decimal places at $\mu = 1/2$ (the numerically evaluated potential, determined using the analytic solution, is correct at least as far as it is given in Table 1). The highly relativistic case $\mu = 3$ can be handled more than satisfactorily by the PN approximation, whereby the potential on the axis is valid to only four decimal places. The accuracy of the series approximation is astonishingly high even for the limit $\mu \rightarrow \mu_0$.⁷ Although the results on the axis are reasonably

comparison to the work of Bardeen and Wagoner.

⁷It should be noted that ρ_0 tends to zero in this limit. The extreme Kerr metric is obtained for $\rho^2 + \zeta^2 \neq 0$, whereas the analytic solution shows that finite values for ξ , as considered here, lead to a different (not asymptotically flat) spacetime (see [9]). The PN approximation, on the other hand, erroneously yields an asymptotically flat spacetime in this limit, at least

	$\mu = 1/2$	$\mu = 3$	$\mu = \mu_0$
$\xi = 1/2,$ $\eta = 1/2$	0.772687415 – 0.022438224 <i>i</i> 0.772687415 – 0.022438224<i>i</i>	–0.281941980 – 0.352810399 <i>i</i> –0.281941981 – 0.352810399<i>i</i>	–0.861419387 – 0.684924117 <i>i</i> –0.861419898 – 0.684924396<i>i</i>
On the axis $\xi = 1,$ $\eta = 1$	0.820284295 – 0.032540154 <i>i</i> 0.820284295 – 0.032540154<i>i</i>	0.127426794 – 0.560328316 <i>i</i> 0.127409032 – 0.560315954<i>i</i>	0 – <i>i</i> –0.006959726 – 0.997783811<i>i</i>
In the disc $\xi = 0,$ $\eta = 3/5$	0.675204587 – 0.041948129 <i>i</i> 0.675204587 – 0.041948129<i>i</i>	–0.626305938 – 0.409718317 <i>i</i> –0.626305488 – 0.409718090<i>i</i>	–1.304973284 – 0.616799888 <i>i</i> –1.304859086 – 0.616728538<i>i</i>

Table 1: The Ernst potential f according to a numerical evaluation of the exact solution in comparison with the results of the PN approximation (bold-faced) up to the order $\mathcal{O}(\mu^{25/2})$ for various points in space and three values of μ .

good in this limit (accurate to within 1%), one can obtain much more accurate results using the Padé approximant. Table 2 provides a comparison of the value of f for a point along the axis returned by the PN series to that of the “diagonal” Padé approximant, whereby diagonal is meant to indicate the approximant for which the polynomial in the numerator is of the same order as the polynomial in the denominator. The values in this table should be compared to the “exact” value found in the cell of the 2nd column and 2nd row of Table 1. It turns out that the values returned by the Padé approximant are so accurate as to provide a viable alternative to numerical methods for all practical purposes.⁸ Using Table 2 one can see, moreover, that the nature of the convergence of the Padé approximation is more uniform and hence more predictable than that of the PN approximation. Thus one could have come up with a good estimate for the accuracy of the Padé values in the table, but not for the PN values. The PN value of order $\mathcal{O}(\mu^{21/2})$, for example, is scarcely more accurate than that of order $\mathcal{O}(\mu^{13/2})$ whereas the corresponding Padé values have won a further 8 decimal places of accuracy. As a rule of thumb, it appears one can rely on the Padé approximant to gain one decimal place of accuracy for each increase of $\sqrt{\mu}$ in the order of the polynomial.

A pictorial impression of the convergence of the PN series can be gleaned from Fig. 2. The proper surface mass density σ_P , which can be calculated from $\sigma_P = \sigma e^{U-k}$ where σ is given by eq. (23) of [2], is divided by Ω to give a dimensionless quantity and plotted as a function of the normalized radius ρ/ρ_0 . A discussion of the curve itself, which lies outside the scope of this paper, can be found in [4]. What is of interest here is the way in which the curves approach the curve (f). Although the tendency to converge can be seen quite clearly, the discrepancy between curves (e) and (f) is fairly large. This is primarily due to

so long as the series is finite.

⁸However, as $\mu \rightarrow \mu_0$, one has to be careful for large ξ .

	$\mathcal{O}(\mu^{9/2})$	$\mathcal{O}(\mu^{13/2})$	$\mathcal{O}(\mu^{17/2})$	$\mathcal{O}(\mu^{21/2})$	$\mathcal{O}(\mu^{25/2})$
PN	0.150938555– 0.564116343 <i>i</i>	0.127710083– 0.556936459 <i>i</i>	0.126549231– 0.561010096 <i>i</i>	0.127627187– 0.560281877 <i>i</i>	0.127409032– 0.560315954 <i>i</i>
Padé	0.140716023– 0.562426687 <i>i</i>	0.127381473– 0.560314135 <i>i</i>	0.127426866– 0.560328310 <i>i</i>	0.127426794– 0.560328316 <i>i</i>	0.127426794– 0.560328316 <i>i</i>

Table 2: The Ernst potential f for $\mu = 3$ at the point $\xi = 1$, $\eta = 1$ according to the PN approximation and the Padé approximant for different orders of the series (cf. 2nd row, 2nd column of the previous table).

the slow convergence of the dimensionless quantity $\Omega\rho_0$. For example, the PN approximation of order $\mathcal{O}(\mu^{25/2})$ returns a value of approximately 0.220 instead of 0.213 for $\Omega\rho_0$ at $\mu = 3$ and at $\mu = 4.5$ the PN approximation yields the grossly erroneous value of 1.46 as compared with the correct value, 1.01×10^{-7} . With the Padé approximant, this problem vanishes and the curves for the proper surface mass density are indistinguishable from the exact curves even at the order $\mathcal{O}(\mu^{9/2})$.

4.3 Ergospheres

The results of Table 1, i.e. the fact that the PN approximation returns a highly accurate value for f even in very relativistic situations, justify the use of this approximation even for the consideration of purely relativistic phenomena. One such phenomenon, the ergosphere, dramatically highlights differences between the Newtonian and Einsteinian theory. An ergosphere is a region in which the Killing vector characterising the stationary nature of the spacetime becomes spacelike (the metric function e^{2U} is negative in this region) so that nothing can remain still relative to an observer at infinity — everything is dragged along by the rotation of the disc.

Figures 3 and 4 depict the ergosphere for two values of μ and calculated for three different orders of the PN approximation (please see [10] for a comparison with ergospheres found by evaluating the analytic solution numerically). One can see in Fig. 3 that the ergosphere for $\mu = 2$, as given by the 6th PN approximation, is nigh on correct, so that higher order terms serve only to refine fine details. In the case of $\mu = 3$, however, (Fig. 4) one can see marked improvement as one moves toward higher orders of the approximation.

As μ increases, the ergosphere moves closer and closer to the axis of rotation where the PN approximation is no longer reliable. This, compounded with the fact that the increasingly poor convergence of the dimensionless quantity $\Omega\rho_0$ as μ nears μ_0 results in scaling problems, leads one to assume that the PN approximation is ill-suited for rendering the ergosphere for values of μ approaching μ_0 . Due to the extreme accuracy of the Padé approximant however, one can indeed divine the nature of the ergospheres even in this limit.

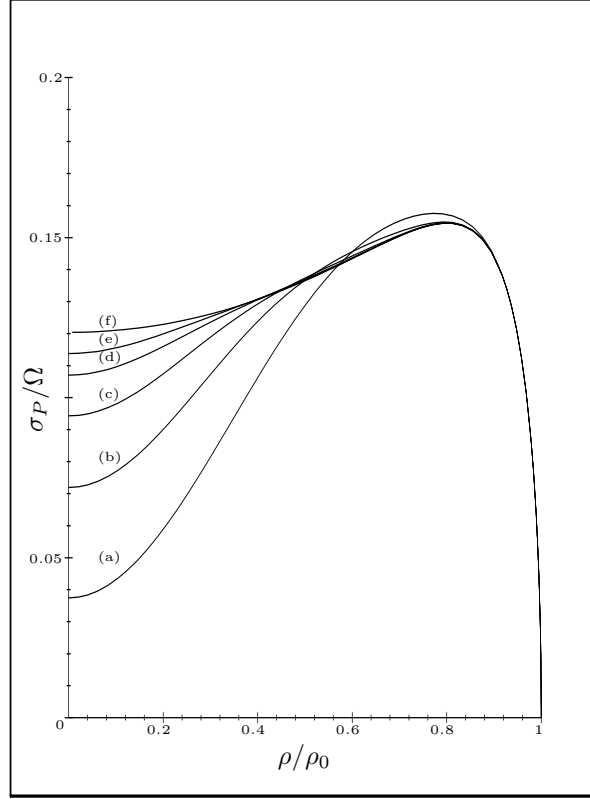


Figure 2: The radial distribution of the proper surface mass density for $\mu = 3$ at different orders of the PN approximation. The curves were created by employing the approximation up to the order (a) $\mathcal{O}(\mu^{9/2})$, (b) $\mathcal{O}(\mu^{13/2})$, (c) $\mathcal{O}(\mu^{17/2})$, (d) $\mathcal{O}(\mu^{21/2})$ and (e) $\mathcal{O}(\mu^{25/2})$. The curve (f) was created by evaluating the exact solution numerically to extremely high accuracy.

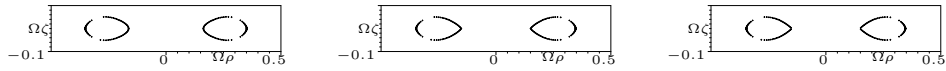


Figure 3: The ergospheres as calculated using the 6th, 8th and 12th PN approximation for $\mu = 2$. The outline represents the curve along which e^{2U} is zero and should be thought of rotated about the axis of symmetry. The inside of the resulting torus-like figure of revolution is then the ergosphere.

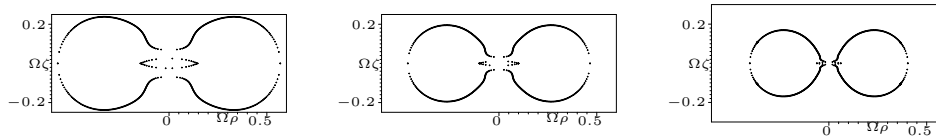


Figure 4: The ergospheres as calculated using the 6th, 8th and 12th PN approximation for $\mu = 3$. The outline represents the curve along which e^{2U} is zero and should be thought of rotated about the axis of symmetry. The inside of the resulting torus-like figure of revolution is then the ergosphere.

5 Conclusion

It was possible, due to the existence of an analytic, global solution for the axially symmetric, stationary, rigidly rotating disc of dust, to come up with an iteration scheme to calculate an arbitrary coefficient in the PN approximation of this solution. This work amounts to the analytic analogue of numerical work published by Bardeen and Wagoner in 1971. The explicit calculation of the expansion coefficients of the Ernst potential was carried out to the 12th PN level (i.e. $\mathcal{O}(\mu^{25/2})$). It turns out that the numerical results from Bardeen and Wagoner are highly accurate for lower orders of the expansion and remain quite good even for higher orders.

The supposition that the PN approximation could be used for many highly relativistic situations was confirmed for the disc of dust, and the very accurate renderings of the ergospheres obtained using the PN approximation attest to the fact that physically meaningful, relativistic phenomena can be studied in some cases using tools tailored to other applications (i.e. to the consideration of the Newtonian regime). It turns out that the position in space to be considered contributes significantly to the convergence of the PN approximation, but not to the convergence of the corresponding Padé approximant. It was found that the PN approximation is unreliable for large μ in the neighbourhood of the axis of rotation even when the approximation is quite accurate elsewhere for the same value of μ , and it can be made highly accurate for all points in space at all values of μ by applying the Padé approximation methods. If one is careful to take into account its limitations, one can use the PN approximation to great advantage for quick and accurate calculations and is bolstered in the opinion that approximation methods can sometimes be extended to applications outside their *a priori* guaranteed region of validity.

References

- [1] G. Neugebauer and R. Meinel, *The Einsteinian Gravitational Field of the Rigidly Rotating Disk of Dust*, *Astrophys. J.* **414**, L97 (1993).

- [2] G. Neugebauer and R. Meinel, *General Relativistic Gravitational Field of a Rigidly Rotating Disk of Dust: Axis Potential, Disk Metric, and Surface Mass Density*, Phys. Rev. Lett. **73**, 2166 (1994).
- [3] G. Neugebauer and R. Meinel, *General Relativistic Gravitational Field of a Rigidly Rotating Disk of Dust: Solution in Terms of Ultraelliptic Functions*, Phys. Rev. Lett. **75**, 3046 (1995).
- [4] J.M. Bardeen and R.V. Wagoner. *Relativistic Disks*. Astrophys. J., **167**, 359 (1971).
- [5] F.J. Ernst. *New Formulation of the Axially Symmetric Gravitational Field Problem*. Phys. Rev., **167**, 1175 (1968).
- [6] D. Petroff. *Das Gravitationsfeld einer rotierenden Scheibe in post-Newtonscher Entwicklung beliebig hoher Ordnung*. Diplomarbeit, Universität Karlsruhe (2000).
- [7] C.M. Bender and S.A. Orszag, *Advanced Mathematical Methods for Scientists and Engineers* (McGraw-Hill, New York, 1978), p. 383.
- [8] T. Damour, B.R. Iyer and B.S. Sathyaprakash, *Improved Filters for Gravitational Waves from Inspiralling Compact Binaries*. Phys. Rev. D **57**, 885 (1998).
- [9] R. Meinel. *The Rigidly Rotating Disk of Dust and its Black Hole Limit in Recent Developments in Gravitation and Mathematical Physics*. Edited by Garcia, Lämmerzahl, Macias, Matos and Nuñez. Science Network Publishing, Konstanz (1998), gr-qc/9703077.
- [10] R. Meinel and A. Kleinwächter. *Dragging Effects near a Rigidly Rotating Disk of Dust*. Einstein Studies (Birkhäuser Boston), **6**, 339 (1995).